



HAL
open science

Complex mode of inheritance in holoprosencephaly revealed by whole exome sequencing

Charlotte Mouden, Christèle Dubourg, Wilfrid Carré, Sophie Rose, Chloé Quélin, Linda Akloul, Géraldine Viot, Houria Salhi, Pierre Darnault, Sylvie Odent, et al.

► **To cite this version:**

Charlotte Mouden, Christèle Dubourg, Wilfrid Carré, Sophie Rose, Chloé Quélin, et al.. Complex mode of inheritance in holoprosencephaly revealed by whole exome sequencing. *Clinical Genetics*, 2016, 89 (6), pp.659-668. 10.1111/cge.12722 . hal-01259228

HAL Id: hal-01259228

<https://hal-univ-rennes1.archives-ouvertes.fr/hal-01259228>

Submitted on 8 Feb 2016

HAL is a multi-disciplinary open access archive for the deposit and dissemination of scientific research documents, whether they are published or not. The documents may come from teaching and research institutions in France or abroad, or from public or private research centers.

L'archive ouverte pluridisciplinaire **HAL**, est destinée au dépôt et à la diffusion de documents scientifiques de niveau recherche, publiés ou non, émanant des établissements d'enseignement et de recherche français ou étrangers, des laboratoires publics ou privés.

Complex mode of inheritance in holoprosencephaly revealed by whole exome sequencing

Charlotte Mouden*¹, Christèle Dubourg*^{1,2}, Wilfrid Carré², Sophie Rose³, Chloé Quelin⁴, Linda Akloul⁴, Géraldine Viot⁵, Houria Salhi⁶, Pierre Darnault⁷, Sylvie Odent^{1,4}, Valérie Dupé¹ and Véronique David^{1,2}

¹UMR6290 Institut de Génétique et Développement de Rennes, Université de Rennes 1, 35043 Rennes, France

²Laboratoire de Génétique Moléculaire et Génomique, C.H.U. de Rennes, 35033 Rennes, France

³UMR1085 Institut de Recherche sur la Santé, l'Environnement et le Travail, Université de Rennes 1, 35043 Rennes, France

⁴Service de Génétique Clinique, C.H.U. de Rennes, 35200 Rennes, France

⁵Service de Génétique Médicale, Maternité Port Royal, 75014 Paris, France

⁶Foetopathologie et Anatomie Pathologique Pédiatrique, Hôpital Cochin, 75014, Paris, France

⁷Service de Radiologie et Imagerie Médicale, C.H.U. de Rennes, 35000 Rennes, France

* Equally contributed to the paper

Corresponding author:

Charlotte Mouden

Charlotte.mouden@univ-rennes1.fr

+33 2 23 23 43 97

IGDR UMR 6290 CNRS, Université de Rennes1,

Faculté de Médecine

2 Avenue du Pr Léon Bernard

35043 Rennes, France

CONFLICT OF INTERESTS STATEMENT

All authors declare that they have no conflicts of interest in the research

ACKNOWLEDGEMENTS

We acknowledge and are extremely grateful to the families who participated in these research studies. We thank the Centre de Ressources Biologiques (CRB-Santé) of Rennes for managing patient samples. We also thank Michelle Ware and Marie de Tayrac for their kind help in editing the manuscript. This work was supported by Agence Nationale de la Recherche (grant no. ANR-12-BSV1-0007-01), Fondation Maladies Rares and Agence de la Biomédecine.

ABSTRACT

Holoprosencephaly (HPE) is the most common congenital cerebral malformation, characterized by impaired forebrain cleavage and midline facial anomalies. Heterozygous mutations in 14 genes have been associated with HPE, and are often inherited from an unaffected parent underlying complex genetic bases. It is now emerging that HPE may result from a combination of multiple genetic events, rather than from a single heterozygous mutation. To explore this hypothesis, we undertook whole exome sequencing (WES) and targeted high-throughput sequencing approaches to identify mutations in HPE subjects. We report here two HPE families in which two mutations are implicated in the disease. In the first family presenting two fetuses with alobar and semi-lobar HPE, we found mutations in two genes involved in HPE, *SHH* and *DISP1*, inherited respectively from the father and the mother. The second reported case is a family with a 9-year old girl presenting lobar HPE, harbouring two compound heterozygous mutations in *DISP1*. Together, these cases of digenic inheritance *SHH/DISP1* and autosomal recessive HPE suggest that in some families, several genetic events are necessary to cause HPE. This study highlights the complexity of HPE inheritance and has to be taken into account by clinicians to improve HPE genetic counseling.

KEY WORDS

DISP1, Holoprosencephaly, Multigenic Inheritance, *SHH*, Whole Exome Sequencing;

INTRODUCTION

Holoprosencephaly (HPE) is the most frequent cerebral malformation, with an occurrence of approximately 1 in 250 embryos and 1.31 in 10,000 births (1). HPE is characterized by a failure to define the midline of the forebrain and midface, with different degrees of severity from a lobar brain to alobar forms associated with cyclopia. Mild manifestations or microforms include ocular hypotelorism, microcephaly and a single central maxillary incisor (2). The mode of inheritance of HPE has been extensively discussed in the literature, and several genetic models have been proposed: autosomal dominant transmission, autosomal recessive transmission or association of mutations in multiple genes (2-5). All these studies point out a strong genetic heterogeneity, with several causative genes identified (Table 1). It mostly implicates heterozygous mutations in *SHH*, *ZIC2*, *SIX3* and *TGIF1*, which are considered as the four major genes involved in HPE. Heterozygous mutations in the minor genes *GLI2*, *PTCH1*, *DISP1*, *FOXH1*, *NODAL*, *TDGF1*, *CDON*, *GAS1*, *DLL1* and *FGF8* have been identified with a lower frequency (2, 6, 7). Recently, two recessive inheritance cases of HPE have been described, implicating mutations in the gene *STIL* (Table 1) (8, 9). Importantly, these genes are all involved in signalling pathways implicated in brain development (4, 9-16) and alteration of SHH signalling appears to be the most common cause of HPE (17).

Although the major genes have been formally involved, their penetrance is usually incomplete with an intra-familial phenotypic variability. Actually, mutations located in these genes are inherited from a parent, asymptomatic or displaying a microform of HPE, in 70% of the cases (2). For example, the same *SHH* mutation can be found in individuals harbouring either alobar HPE or minor forms (18). Consequently, the clinical variability could be due to abnormalities in other genes that have a function in the same or interacting signalling pathways (19, 20).

This is strongly supported by the description of mouse models carrying mutations in two genes of the same or different signalling pathways. For example, whereas *Gas1*^{-/-} mutant mice exhibit partial fusion of the medial nasal processes and *Shh*^{+/-} mice appear normal, *Gas1*^{-/-};*Shh*^{+/-} mice embryos display complete fusion of the medial nasal processes (21), reminiscent of a HPE phenotype. Such examples of animal models are numerous and all

support the hypothesis that HPE could be due to a cumulative partial inhibition of signalling pathways implicated in forebrain development (6, 22).

However, there are only a few examples in the literature that suggest that HPE could be related to combined failures of several HPE genes in human (Table 2), including patients with co-occurring mutations or deletions in *SHH/TGIF1* and *SHH/ZIC2* (23). Nevertheless, sequencing of the four major genes (*SHH*, *ZIC2*, *TGIF1*, *SIX3*) in large HPE cohorts has not allowed to validate this hypothesis (2, 5, 14). Thus, the mode of inheritance of HPE is still unclear.

Identifying more genes in families in which polygenic inheritance is suspected would be very beneficial to understand the pathogenic mechanism of this developmental disorder. This is now facilitated by the recent development of next generation sequencing technologies (20). In this study, we performed whole exome sequencing (WES) in a family where the father carries a mutation in *SHH*, transmitted to 3 fetuses with semi-lobar and alobar HPE. We hypothesized that the fetuses have all inherited a second mutation in another gene from the mother. This original strategy was powerful as it revealed a second mutation in *DISP1* shared by the mother and the HPE fetuses. This family is the first one in which mutations in the two HPE-associated genes, *SHH* and *DISP1*, have been identified. Furthermore using a targeted NGS method, the involvement of *DISP1* in HPE was reinforced by the observation of two *DISP1* compound heterozygous mutations in another HPE family. These results support the complexity of HPE inheritance and raise important questions about how clinicians should consider the inheritance mode of HPE.

MATERIALS AND METHODS

Patients and samples

Patients presenting midline abnormalities and suspicion of holoprosencephaly were referred from the Centre Hospitalier Universitaire of Rennes (France) and the Hôpital Cochin (Paris, France) through the network of reference centres for developmental anomalies and malformation syndromes (CLAD centres). Patients and parents blood and tissue samples were obtained from the processing of biological samples through the Centre de Ressources Biologiques (CRB) Santé of Rennes BB-0033-00056 (<http://www.crbsante-rennes.com>). The research protocol was conducted under French legal guidelines and fulfilled the requirements

of the local institutional ethics committee. The parents of the photographed patient assented to include photographs in a scientific publication.

F1 family

The mother II2 had three terminations of pregnancy with fetuses (III1, III2 and III3) harbouring semi-lobar or alobar HPE (Fig. 1a and Table 3a). The F1 family also includes two other healthy girls III4 and III5, being 12 and 11 years old respectively. The father II1, the grandfather I1 and the uncle II3 all present microcephaly. This latter had 4 children among which 3 (III6, III7 and III9) harbour microcephaly and minor facial midline malformations (hypotelorism). The father II1 also had two healthy siblings, II5 and II6 (Table 3a). DNA was available for all family members except II4.

F2 family

The F2 family includes three members, the two healthy parents I1 and I2 and their 9-year old girl III1 who displayed a lobar HPE (Fig. 2 and Table 3b). She has two healthy siblings but their DNA was not available. Pregnancy was normal. A wide cleft palate was observed at birth, which was surgically treated. III1 was then referred to genetic counselling at 5-and-half-years old for psychomotor retardation (started walking at 21 months and had a language delay) and learning difficulties. On clinical examination, she weighed 16.5 kg (-1 standard deviation), was 109.5 cm tall, and had microcephaly (-2SD). She presented facial dysmorphism with flat face, short nose, small mouth and hypotelorism (Figs. 2c and 2d). At the sight of these clinical observations, we recommended a molecular diagnosis of HPE. Molecular testing of 18 HPE genes was performed on DNA of the daughter III1, revealing the presence of two compound heterozygous mutations in the minor HPE gene *DISP1*. Subsequently, to confirm the presence of HPE, MRI was performed and showed a mild form of lobar HPE with a very localized fusion of hemispheres in the forebrain (Fig. 2b).

Whole Exome Sequencing

WES was performed by the Genoscope on the DNA of the two parents III1 and II2 and one of the fetuses III2 in F1 family, using “SeqCap EZ Exome v3.0” capture (Roche) on HiSeq™2000 platform (Illumina). Exomes were homogeneously sequenced with a mean coverage of 93% of the targeted bases with read depth greater than 20X, and an overall mean

depth of coverage of 112X. Bioinformatic analyses were conducted with the Illumina pipeline analysis CASAVA 1.8. The sequenced reads were aligned on the reference human genome 19 (hg19) with Eland v2.0 before variant calling (SNV and INDEL) with the CASAVA suite. Resulting variants were annotated using ANNOVAR v2.0 (http://www.openbioinformatics.org/annovar/annovar_filter.html). Variants population frequencies were extracted from three different public databases (the Exome Sequencing Project (ESP6500), the 1000 Genomes Project (1000g, 2014) and the Exome Aggregation Consortium (ExAC02)). Several bioinformatics predictions tools were used to predict conservation (GERP++, PhyloP, SiPhy, and PhastCons Elements 46-way) (24-27) and deleterious effect of SNVs and INDELS (SIFT, PolyPhen-2 HDIV and HVAR, LRT, Mutation Taster, Mutation Assessor, FATHMM, Radial SVM, LR and CADD) (28-34). Visual inspection of candidate variants was performed with Integrative Genome Viewer (IGV, Broad Institute).

Targeted high-throughput sequencing

Targeted NGS was performed using Ion Torrent technology (Life Technologies) on DNA from the girl III in F2 family. Two pools of 711 primer pairs were designed (Ion Ampliseq technology, Life Technologies) to sequence all the exons of a panel of 18 genes involved in HPE or candidates (*SHH*, *ZIC2*, *TGIF1*, *SIX3*, *DISP1*, *CDON*, *GAS1*, *SUFU*, *FGF8*, *FGFR1*, *NODAL*, *HHAT*, *SUFU*, *TDGF1*, *PTCH1*, *FOXH1*, *SOX2*, *DLL1*) and 2 *SHH* expression regulatory regions, spanning 111kb. Libraries were sequenced with Ion PGMTM System (Life Technologies). A PGM-specific pipeline incorporated in the Ion Torrent server (Torrent Suite version 4.0.2; Life Technologies) was used to perform the following steps: reads alignment on hg19, targeted regions coverage analysis, filtering and removal of poor signal reads. Variant calling was performed with the Ion Torrent Variant Caller version 4.0. Mutations were annotated using ANNOVAR v2.0 as described for WES analysis and with Alamut software (Interactive Biosoftware).

Sanger sequencing

Sanger sequencing in F1 and F2 families assessed the intrafamilial segregation of the candidate mutations found by NGS. This was done using the BigDye terminator cycle sequencing kit (Applied Biosystems) on an ABI3130xl sequencer (Applied Biosystems) and analysed using SeqScape software v2.6 (Life Technologies).

Functional validation of the *SHH* p.Pro347Gln mutation

The human *SHH* cDNA (RefSeq NM_000193) was cloned in a pMSCVneo (Clontech) vector. A mutated plasmid containing the *SHH* p.Pro347Gln mutation was obtained by site-directed mutagenesis using the QuikChange XL Site-directed Mutagenesis Kit (Stratagene, La Jolla, USA). Plasmids containing cDNA of *SHH* WT or *SHH* p.Pro347Gln were transfected in C3H10T1/2 cells using Transfast (Promega). Six days later, the alkaline phosphatase activity was measured as previously described (35), reliable to the differentiation of C3H10T1/2 into osteoblasts under SHH action.

RESULTS

F1 family

In the F1 family, we showed by Sanger sequencing that a p.Pro347Gln mutation in *SHH* (c.1040C>A of RefSeq NM_000193) was present in fetuses III1, III2 and III3 inherited from the father II1 (Fig. 1a). It was inherited from the grandfather I1, and was also transmitted to the uncle II3, displaying microcephaly and hypotelorism. This uncle transmitted the *SHH* mutation to 3 children (III6, III7 and III9), also harbouring microcephaly and hypotelorism. WES analysis validated the known heterozygous *SHH* mutation in the father II1 presenting microcephaly and hypotelorism, and in the HPE fetus III2.

The deleterious effect of the *SHH* p.Pro347Gln mutation was evaluated using an adaptation of a cell-based assay previously described (35). The efficiency of SHH signalisation in presence of the mutation was evaluated by quantifying the SHH-dependent differentiation of mesenchymal cells (C3H10T1/2) into osteoblasts. This was assessed by measuring the activity of the alkaline phosphatase (ALP) in C3H10T1/2 cells, 6 days after transfection with the pMSCVneo plasmids containing either cDNA of *SHH* WT or cDNA of *SHH* p.Pro347Gln. The ALP activity of the cells expressing the mutated *SHH* was 0,04 μU by μg of protein extract, while it was 1.31 $\mu\text{U}/\mu\text{g}$ in the protein extract from cells expressing *SHH* WT, meaning that C3H10T1/2 cells failed to undergo osteoblastic differentiation under action of mutated SHH. This strongly reflects the deleteriousness of the p.Pro347Gln mutation (Fig. 1b).

Based on the assumption that HPE observed in the fetus III2 resulted from the association of the *SHH* mutation with another mutation, variants were filtered according to this inheritance pattern. Only mutations inherited from the mother I2 were selected in the child III2. Intronic variants were filtered out, as well as synonymous variants and those that had a population allele frequency over 1% in any of the three public databases 1000g, ESP6500, and ExAC02. Thirty-four variants were selected, and a prioritization was performed using the cumulative predictions of ten bioinformatics tools. The 10 first-ranked candidate mutations are presented in supplementary data (Fig. S1). Most of these genes were already associated with genetic syndromes without any obvious link with forebrain development. We thus focused on a mutation in *DISP1*, known to be involved in HPE. This mutation is a substitution of a thymine in cytosine at location c.3287 of *DISP1* (NM_032890), leading to the change of a methionine in threonine at location p.1096. This mutation was listed as rs144673025 in dbSNP database, and has a minor allele frequency of 0,55% in ESP6500, 0,1398% in 1000g, and 0,6189% in ExAC02. Three bioinformatics prediction tools classified this mutation as deleterious (LRT, Mutation Taster, and FATHMM) while other tools predicted it as tolerated (PolyPhen-2, SIFT, radial SVM, LR, and Mutation Assessor) (Table 4).

We used Sanger sequencing to search for the *DISP1* c.3287T>C mutation in individuals III3, III4 and III5 (Fig. 1). DNA was no longer available to look for this *DISP1* mutation in fetus III1. A perfect co-segregation of the two mutations, *SHH* p.Pro347Gln and *DISP1* p.Met1096Thr was observed in HPE fetuses III2 and III3. Among the two healthy sisters, III4 has no mutation whereas III5 carries the *DISP1* mutation only.

F2 family

The F2 family was screened for 18 HPE candidate genes using targeted NGS for molecular diagnosis on the DNA of the daughter III1. Two heterozygous mutations were identified in the exon 10 of *DISP1*: the c.1087A>G transition leading to a missense mutation p.Asn363Asp and the c.1657G>A transition leading to a missense mutation p.Glu553Lys. Sanger sequencing on DNA of the parents showed that the p.Asn363Asp mutation was inherited from the father I1, and the p.Glu553Lys mutation was inherited from the mother I2 (Fig. 2a).

The *DISP1* p.Asn363Asp mutation was absent from public databases, and was predicted deleterious by 7 out of 10 of the prediction tools employed. The second mutation, p.Glu553Lys, was also predicted deleterious by the majority of the prediction tools, and was also absent from public sequencing databases (Table 4). According to the Alamut software

and the other conservation scores used, these two mutations were in highly conserved regions at both the nucleotide and the amino acid level.

DISCUSSION

The genetic heterogeneity of HPE is supported by reduced penetrance and the absence of obvious genotype-phenotype correlation. This is especially true for patients carrying heterozygous *SHH* mutations, as 45% harbor microforms, 45% present severe HPE and 10% are apparently asymptomatic (18). Using WES, we report here the first co-segregation of mutations in *SHH* and *DISP1* with severe HPE. Our results suggest that these mutations are combining to give a severe phenotype and provide strong evidence that digenic inheritance is a significant genetic model for HPE.

Relationships between *SHH* and *DISP1* in HPE

In this study, we have investigated one family carrying a deleterious mutation in *SHH* and displaying variable expressivity of the disease. This mutation causes the change of proline in glutamine, which results in a severe reduction of SHH activity. Although microcephaly is not a typical sign of HPE, we can consider that the *SHH* mutation is responsible for this mild form of HPE in the present family (2). *SHH* mutation shows full penetrance with microcephaly whereas a second mutation in *DISP1* seems to be necessary to obtain a more severe HPE in 3 fetuses. This is also supported by the finding that the mother and a clinically normal sister carried only the mutation in *DISP1*.

In this study we also describe the first HPE case with compound heterozygous mutations in *DISP1*. Altogether, we find 3 different mutations (Fig. 3) in conserved regions of *DISP1*, including one in the Sterol Sensing Domain (SSD). The exact role of the SSD remains unclear, although most SSD containing proteins have been implicated in intracellular trafficking (36, 37). These 3 missense mutations in *DISP1* provide new arguments for the implication of this gene in HPE. Few other mutations in *DISP1* have been previously described in patient only harbouring microforms of HPE (38, 39). Noteworthy, all these *DISP1* mutations were inherited from clinically unaffected parents. This gives evidence that additional factors are necessary to potentiate these mutations of *DISP1* and to lead to HPE. As *DISP1* mediates the secretion of SHH from producing cells, and allows consequent paracrine signalling (40), we hypothesized that these mutations have an impact on SHH signalling.

Mice data also strongly reveal the implication of *Disp1* in HPE (40-42). Heterozygous knockout for *Disp1* are undistinguishable from the wildtype whereas *Disp1*^{-/-} embryos do not survive beyond E9.5 because of heart development defects. They also display cyclopia reminiscent to severe HPE (43). Further analysis of these mutants permitted to show that Shh signalling was disrupted in *Disp1*^{-/-} embryos, indicating that *Disp1* is essential for proper Shh signalling. Thus, *Disp1* is most probably critical for ventral forebrain induction through its interaction with Shh pathway. Consequently, the co-segregation of a mutation in *SHH* and a mutation in *DISP1* with severe HPE strongly suggests that cumulative effects lead to severe impairment of forebrain development.

Inheritance in HPE

Some authors have proposed autosomal recessive inheritance in HPE (3, 44). However, despite systematic sequencing, homozygous mutations in the major HPE genes *SHH*, *ZIC2* and *SIX3*, were never described in HPE cohorts (2, 5, 45). Nonetheless some autosomal recessive cases implicating minor HPE genes (Table 1) have been reported. In 2007, a first case of recessive inheritance of *TGIF1* mutations was described, with the finding of two compound heterozygous mutations (46). A loss of function homozygous mutation in *FGF8* has also been identified in one consanguineous HPE family (47). More recently, hypomorphic alleles of *STIL* were implicated in two cases of autosomal recessive inheritance in HPE patients (8, 9). It was proposed that *STIL* had a function during early brain development linked to SHH signalling (9, 48). Here, we describe a first HPE patient displaying two mutated *DISP1* alleles whereas the two clinically normal parents carry only one mutated allele. This strongly supports that the presence of two mutations in a minor HPE gene exacerbates the risk of developing a HPE phenotype. Furthermore, the mild phenotype of the HPE patient described in this manuscript suggests that DISP1 activity is decreased such that it leads to a significant impairing of SHH pathway responsible for mild HPE, but above the threshold that would result in severe HPE and early lethality, as indicated by the mice model (43).

Currently, single heterozygous mutations are mainly reported in HPE cases (Table 1) and believed to account for the HPE phenotype (5). But still, it cannot be excluded that a mutation in another gene may underlie the observed forebrain defects. However, double heterozygous mutations for two HPE genes were rarely reported (Table 2). This is not really surprising because HPE genes are key developmental genes, and strong deleterious mutations in two of

these genes are probably not viable (44, 49). Thus, it is important to design the pipeline of WES analysis in order to avoid discarding mutations predicted to have a mildly deleterious effect in development genes. This strategy has enabled us to identify a new *DISP1* mutation in a family presenting two fetuses with alobar and semi-lobar HPE associated to a deleterious mutation in *SHH*. The identification of these two altered genes that have functional relationships in multiple affected individuals in one family strongly supports a digenic inheritance (19).

Polygenic inheritance has now been established for more and more other complex inheritance diseases among which digenic inheritance is the simplest form (19, 20). This mode of inheritance was reported in Kallmann syndrome (KS) (50), characterized by a defective hormonal reproductive axis and sense of smell. This developmental pathology was firstly described as autosomal dominant or X chromosome-linked. Further studies permitted to refine the genetics of KS syndrome by describing several patients harbouring two mutations in different genes (51, 52), combining major and minor KS genes, and giving evidence of a digenic inheritance of KS syndrome. This was also reported in patients with Alport syndrome, presenting mutations in two different collagen IV genes (*COL4A3* and *COL4A4*) (53). In some nephropathies, mutations in two genes encoding glomerular proteins nephrin and podocin (*NPHS1* and *NPHS2*) were identified in several patients (54). Such a multigenic inheritance is also well described in ciliopathies like Bardet-Biedl syndrome (BBS) with many patients harbouring mutations in two or more *BBS* genes (55). These cases illustrate how, in complex syndromes with variable severity, polygenic inheritance plays a role in the clinical expression of the disease. This is particularly relevant when there is functional relationships between mutated genes, as this is the case for HPE genes (44). A first online database dedicated to digenic diseases (DIDA, <http://dida.ibsquare.be/>) is now available (20). The cases described in our manuscript fully meet the required criteria to be included in DIDA database (20).

By describing new HPE families with no classical autosomal dominant inheritance, our work refines the genetic bases of HPE. This discovery has significant implications for genetic counseling especially for risk assessment of patient relatives. Clinical geneticists have to be aware of such different patterns of heritability, and WES or at least sequencing of a large panel of HPE genes, should be performed to establish a molecular diagnosis.

REFERENCES

1. Leoncini E, Baranello G, Orioli IM et al. Frequency of holoprosencephaly in the International Clearinghouse Birth Defects Surveillance Systems: searching for population variations. *Birth Defects Res A Clin Mol Teratol* 2008; 82: 585-591.
2. Mercier S, Dubourg C, Garcelon N et al. New findings for phenotype-genotype correlations in a large European series of holoprosencephaly cases. *J Med Genet* 2011; 48: 752-760.
3. Barr M, Jr., Cohen MM, Jr. Autosomal recessive alobar holoprosencephaly with essentially normal faces. *Am J Med Genet* 2002; 112: 28-30.
4. Ming JE, Kaupas ME, Roessler E et al. Mutations in PATCHED-1, the receptor for SONIC HEDGEHOG, are associated with holoprosencephaly. *Hum Genet* 2002; 110: 297-301.
5. Roessler E, Velez JI, Zhou N, Muenke M. Utilizing prospective sequence analysis of SHH, ZIC2, SIX3 and TGIF in holoprosencephaly probands to describe the parameters limiting the observed frequency of mutant gene-gene interactions. *Mol Genet Metab* 2012; 105: 658-664.
6. Mercier S, David V, Ratié L et al. NODAL and SHH dose-dependent double inhibition promotes an HPE-like phenotype in chick embryos. *Dis Model Mech* 2013; 6: 537-543.
7. Solomon BD, Gropman A, Muenke M. Holoprosencephaly Overview. In: Pagon RA, Adam MP, Ardinger HH et al., eds. *GeneReviews*(R). Seattle (WA), 1993.
8. Kakar N, Ahmad J, Morris-Rosendahl DJ et al. STIL mutation causes autosomal recessive microcephalic lobar holoprosencephaly. *Hum Genet* 2015; 134: 45-51.
9. Mouden C, de Tayrac M, Dubourg C et al. Homozygous STIL Mutation Causes Holoprosencephaly and Microcephaly in Two Siblings. *Plos One* 2015; 10: e0117418.
10. De La Cruz JM, Bamford RN, Burdine RD et al. A loss-of-function mutation in the CFC domain of TDGF1 is associated with human forebrain defects. *Hum Genet* 2002; 110: 422-428.
11. Arauz RF, Solomon BD, Pineda-Alvarez DE et al. A hypomorphic allele in the FGF8 gene contributes to holoprosencephaly and is allelic to gonadotropin-releasing hormone deficiency in humans. *Mol Syndromol* 2010; 1: 59-66.
12. Ribeiro LA, Queizi RG, Nascimento A, Bertolacini CP, Richieri-Costa A. Holoprosencephaly and holoprosencephaly-like phenotype and GAS1 DNA sequence changes: Report of four Brazilian patients. *Am J Med Genet* 2010; 152: 1688-1694.
13. Bae GU, Domené S, Roessler E et al. Mutations in CDON, encoding a hedgehog receptor, result in holoprosencephaly and defective interactions with other hedgehog receptors. *Am J Hum Genet* 2011; 89: 231-240.
14. Dubourg C, David V, Gropman A et al. Clinical utility gene card for: Holoprosencephaly. *Eur J Hum Genet* 2011; 19: preceeding 118-120.
15. Dupé V, Rochard L, Mercier S et al. NOTCH, a new signaling pathway implicated in holoprosencephaly. *Hum Mol Genet* 2011; 20: 1122-1131.
16. Ratié L, Ware M, Barloy-Hubler F et al. Novel genes upregulated when NOTCH signalling is disrupted during hypothalamic development. *Neural Dev* 2013; 8: 25.
17. Cohen MM, Jr. Hedgehog signaling update. *Am J Med Genet A* 2010; 152A: 1875-1914.
18. Solomon BD, Bear Ka, Wyllie a et al. Genotypic and phenotypic analysis of 396 individuals with mutations in Sonic Hedgehog. *J Med Genet* 2012; 49: 473-479.
19. Schaffer AA. Digenic inheritance in medical genetics. *J Med Genet* 2013; 50: 641-652.
20. Gazzo AM, Daneels D, Cilia E et al. DIDA: A curated and annotated digenic diseases database. *Nucleic Acids Res* 2015.
21. Allen BL, Tenzen T, McMahon AP. The Hedgehog-binding proteins Gas1 and Cdo cooperate to positively regulate Shh signaling during mouse development. *Genes Dev* 2007; 21: 1244-1257.
22. Krauss RS. Holoprosencephaly: new models, new insights. *Expert Rev Mol Med* 2007; 9: 1-17.

23. Nanni L, Ming JE, Bocian M et al. The mutational spectrum of the Sonic Hedgehog gene in holoprosencephaly: SHH mutations cause a significant proportion of autosomal dominant holoprosencephaly. *Hum Mol Genet* 1999; 8: 2479-2488.
24. Siepel A, Bejerano G, Pedersen JS et al. Evolutionarily conserved elements in vertebrate, insect, worm, and yeast genomes. *Genome Res* 2005; 15: 1034-1050.
25. Garber M, Guttman M, Clamp M et al. Identifying novel constrained elements by exploiting biased substitution patterns. *Bioinformatics* 2009; 25: 54-62.
26. Davydov EV, Goode DL, Sirota M et al. Identifying a high fraction of the human genome to be under selective constraint using GERP++. *PLoS Comput Biol* 2010; 6.
27. Pollard KS, Hubisz MJ, Rosenbloom KR, Siepel A. Detection of nonneutral substitution rates on mammalian phylogenies. *Genome Res* 2010; 20: 110-121.
28. Ng PC, Henikoff S. Predicting deleterious amino acid substitutions. *Genome Res* 2001; 11: 863-874.
29. Chun S, Fay JC. Identification of deleterious mutations within three human genomes. *Genome Res* 2009; 15: 1553-1561.
30. Reva B, Antipin Y, Sander C. Predicting the functional impact of protein mutations: Application to cancer genomics. *Nucleic Acids Res* 2011; 39: 37-43.
31. Adzhubei I, Jordan DM, Sunyaev SR. Predicting Dunctional Effect of Human Missense Mutations Using PolyPhen-2. *Curr Protoc Hum Genet* 2013; 7.
32. Shihab Ha, Gough J, Cooper DN et al. Predicting the functional, molecular, and phenotypic consequences of amino acid substitutions using hidden Markov models. *Hum Mutat* 2013; 34: 57-65.
33. Dong C, Wei P, Jian X et al. Comparison and integration of deleteriousness prediction methods for nonsynonymous SNVs in whole exome sequencing studies. *Hum Mol Genet* 2014; 24: 2125-2137.
34. Kircher M, Witten DM, Jain P et al. A general framework for estimating the relative pathogenicity of human genetic variants. *Nat Genet* 2014; 46: 310-315.
35. Traiffort E, Dubourg C, Faure H et al. Functional characterization of Sonic Hedgehog mutations associated with holoprosencephaly. *J Biol Chem* 2004; 279: 42889-42897.
36. Kuwabara PE, Labouesse M. The sterol-sensing domain: Multiple families, a unique role? *Trends Genet* 2002; 18: 193-201.
37. Nakano Y, Kim HR, Kawakami a et al. Inactivation of dispatched 1 by the chameleon mutation disrupts Hedgehog signalling in the zebrafish embryo. *Dev Biol* 2004; 269: 381-392.
38. Roessler E, Ma Y, Ouspenskaia MV et al. Truncating loss-of-function mutations of DISP1 contribute to holoprosencephaly-like microform features in humans. *Hum Genet* 2009; 125: 393-400.
39. Kantarci S, Ackerman KG, Russel MN et al. Characterization of the chromosome 1q41q42.12 region, and the candidate gene DISP1, in patients with CDH. *Am J Med Genet* 2010; 10: 2493-2504.
40. Tian H, Jeong J, Harfe BD, Tabin CJ, McMahon AP. Mouse *Disp1* is required in sonic hedgehog-expressing cells for paracrine activity of the cholesterol-modified ligand. *Development (Cambridge, England)* 2005; 132: 133-142.
41. Kawakami T, Kawcak T, Li YJ et al. Mouse dispatched mutants fail to distribute hedgehog proteins and are defective in hedgehog signaling. *Development* 2002; 129: 5753-5765.
42. Caspary T, Garcia-Garcia MJ, Huangfu D et al. Mouse Dispatched homolog1 is required for long-range, but not juxtacrine, Hh signaling. *Curr Biol* 2002; 12: 1628-1632.

43. Kawakami T, Kawcak TN, Li Y-J et al. Mouse dispatched mutants fail to distribute hedgehog proteins and are defective in hedgehog signaling. *Development (Cambridge, England)* 2002; 129: 5753-5765.
44. Cohen MM, Jr. Holoprosencephaly: clinical, anatomic, and molecular dimensions. *Birth Defects Res A Clin Mol Teratol* 2006; 76: 658-673.
45. Dubourg C, Lazaro L, Pasquier L et al. Molecular screening of SHH, ZIC2, SIX3, and TGIF genes in patients with features of holoprosencephaly spectrum: Mutation review and genotype-phenotype correlations. *Hum Mutat* 2004; 24: 43-51.
46. El-Jaick KB, Powers SE, Bartholin L et al. Functional analysis of mutations in TGIF associated with holoprosencephaly. *Mol Cell Biol* 2007; 90: 97-111.
47. McCabe MJ, Gaston-Massuet C, Tziaferi V et al. Novel FGF8 mutations associated with recessive holoprosencephaly, craniofacial defects, and hypothalamo-pituitary dysfunction. *J Clin Endocrinol Metab* 2011; 96: E1709-1718.
48. David A, Liu F, Tibelius A et al. Lack of centrioles and primary cilia in *STIL*^{-/-} mouse embryos. *Cell Cycle* 2014; 13: 2859-2868.
49. Roessler E, Muenke M. The molecular genetics of holoprosencephaly. *Am J Med Genet C Semin Med Genet* 2010; 154C: 52-61.
50. Klein VR, Friedman JM, Brookshire GS, Brown OE, Edman CD. Kallmann syndrome associated with choanal atresia. *Clin Genet* 1987; 31: 224-227.
51. Canto P, Munguia P, Soderlund D, Castro JJ, Mendez JP. Genetic analysis in patients with Kallmann syndrome: coexistence of mutations in prokineticin receptor 2 and KAL1. *J Androl* 2009; 30: 41-45.
52. Dode C, Hardelin JP. Clinical genetics of Kallmann syndrome. *Ann Endocrinol (Paris)* 2010; 71: 149-157.
53. Mencarelli Ma, Heidet L, Storey H et al. Evidence of digenic inheritance in Alport syndrome. *J Med Genet* 2015; 52: 163-174.
54. Koziell A, Grech V, Hussain S et al. Genotype/phenotype correlations of NPHS1 and NPHS2 mutations in nephrotic syndrome advocate a functional inter-relationship in glomerular filtration. *Hum Mol Genet* 2002; 11: 379-388.
55. Katsanis N, Eichers ER, Ansley SJ et al. BBS4 is a minor contributor to Bardet-Biedl syndrome and may also participate in triallelic inheritance. *Am J Hum Genet* 2002; 71: 22-29.
56. Roessler E, Belloni E, Gaudenz K et al. Mutations in the human Sonic Hedgehog gene cause holoprosencephaly. *Nat Genet* 1996; 14: 357-360.
57. Roessler E, Belloni E, Gaudenz K et al. Mutations in the C-terminal domain of Sonic Hedgehog cause holoprosencephaly. *Hum Mol Genet* 1997; 6: 1847-1853.
58. Heussler HS, Suri M, Young ID, Muenke M. Extreme variability of expression of a Sonic Hedgehog mutation: attention difficulties and holoprosencephaly. *Arch Dis Child* 2002; 86: 293-296.
59. Brown SA, Warburton D, Brown LY et al. Holoprosencephaly due to mutations in ZIC2, a homologue of *Drosophila* odd-paired. *Nat Genet* 1998; 20: 180-183.
60. Orioli IM, Castilla EE, Ming JE et al. Identification of novel mutations in SHH and ZIC2 in a South American (ECLAMC) population with holoprosencephaly. *Hum Genet* 2001; 109: 1-6.
61. Solomon BD, Lachawan F, Mercier S et al. Mutations in ZIC2 in human holoprosencephaly: description of a novel ZIC2 specific phenotype and comprehensive analysis of 157 individuals. *J Med Genet* 2010; 47: 513-524.
62. Ramocki MB, Scaglia F, Stankiewicz P et al. Recurrent partial rhombencephalosynapsis and holoprosencephaly in siblings with a mutation of ZIC2. *Am J Med Genet A* 2011; 155A: 1574-1580.

63. Wallis DE, Roessler E, Hehr U et al. Mutations in the homeodomain of the human SIX3 gene cause holoprosencephaly. *Nat Genet* 1999; 22: 196-198.
64. Pasquier L, Dubourg C, Blayau M et al. A new mutation in the six-domain of SIX3 gene causes holoprosencephaly. *Eur J Hum Genet* 2000; 8: 797-800.
65. Ribeiro LA, El-Jaick KB, Muenke M, Richieri-Costa A. SIX3 mutations with holoprosencephaly. *Am J Med Genet A* 2006; 140: 2577-2583.
66. Lacbawan F, Solomon BD, Roessler E et al. Clinical spectrum of SIX3-associated mutations in holoprosencephaly: correlation between genotype, phenotype and function. *J Med Genet* 2009; 46: 389-398.
67. Hehr U, Pineda-Alvarez DE, Uyanik G et al. Heterozygous mutations in SIX3 and SHH are associated with schizencephaly and further expand the clinical spectrum of holoprosencephaly. *Hum Genet* 2010; 127: 555-561.
68. Gripp KW, Wotton D, Edwards MC et al. Mutations in TGIF cause holoprosencephaly and link NODAL signalling to human neural axis determination. *Nat Genet* 2000; 25: 205-208.
69. Aguilera C, Dubourg C, Attia-Sobol J et al. Molecular screening of the TGIF gene in holoprosencephaly: identification of two novel mutations. *Hum Genet* 2003; 112: 131-134.
70. Rahimov F, Ribeiro LA, de Miranda E, Richieri-Costa A, Murray JC. GLI2 mutations in four Brazilian patients: how wide is the phenotypic spectrum? *Am J Med Genet A* 2006; 140: 2571-2576.
71. Ribeiro LA, Murray JC, Richieri-Costa A. PTCH mutations in four Brazilian patients with holoprosencephaly and in one with holoprosencephaly-like features and normal MRI. *Am J Med Genet A* 2006; 140: 2584-2586.
72. Roessler E, Du YZ, Mullor JL et al. Loss-of-function mutations in the human GLI2 gene are associated with pituitary anomalies and holoprosencephaly-like features. *Proc Natl Acad Sci U S A* 2003; 100: 13424-13429.
73. Bertolacini CD, Ribeiro-Bicudo LA, Petrin A, Richieri-Costa A, Murray JC. Clinical findings in patients with GLI2 mutations--phenotypic variability. *Clin Genet* 2012; 81: 70-75.
74. Roessler E, Ouspenskaia MV, Karkera JD et al. Reduced NODAL signaling strength via mutation of several pathway members including FOXH1 is linked to human heart defects and holoprosencephaly. *Am J Hum Genet* 2008; 83: 18-29.
75. Roessler E, Pei W, Ouspenskaia MV et al. Cumulative ligand activity of NODAL mutations and modifiers are linked to human heart defects and holoprosencephaly. *Mol Genet Metab* 2009; 98: 225-234.
76. Bennett H, Presti A, Adams D et al. A prenatal presentation of severe microcephaly and brain anomalies in a patient with novel compound heterozygous mutations in the STIL gene found postnatally with exome analysis. *Pediatr Neurol* 2014; 51: 1-3.
77. Lacbawan F, Solomon BD, Roessler E et al. Clinical spectrum of SIX3-associated mutations in holoprosencephaly: correlation between genotype, phenotype and function. *J Med Genet* 2009; 46: 389-398.

LEGENDS

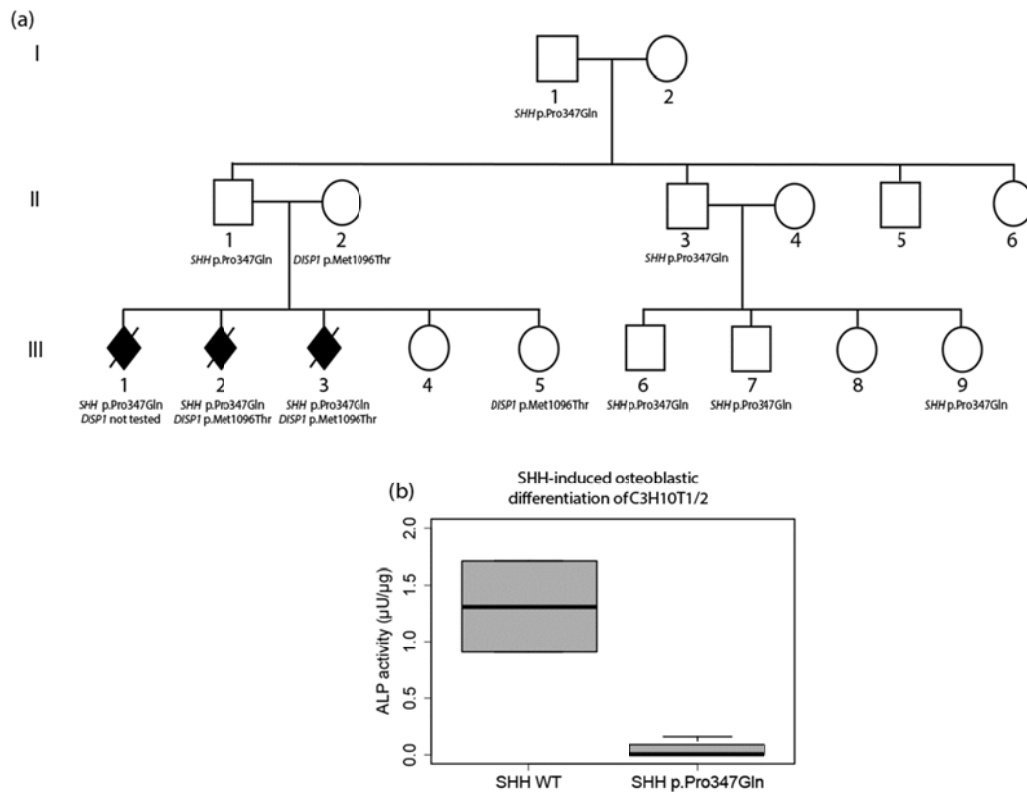


Figure 1. Pedigree of F1 family and functional test of the *SHH* p.Pro347Gln mutation

(a) Black symbols refer to HPE subjects. Mutations were represented in proteic nomenclature. The F1 family consisted of 17 members. Nine of them harbor the *SHH* p.Pro347Gln mutation, inherited from the paternal grand-father II1. In addition to the *SHH* mutation, fetuses III2 and III3 have a *DISP1* p.Met1096Thr mutation, transmitted by their mother II2. The fetus III1 was not tested for *DISP1*, as DNA quantity was insufficient. (b) Alkaline Phosphatase (ALP) activity measured in total protein extracts from C3H10T1/2 cells transfected with plasmids containing *SHH* WT or *SHH* p.Pro347Gln.

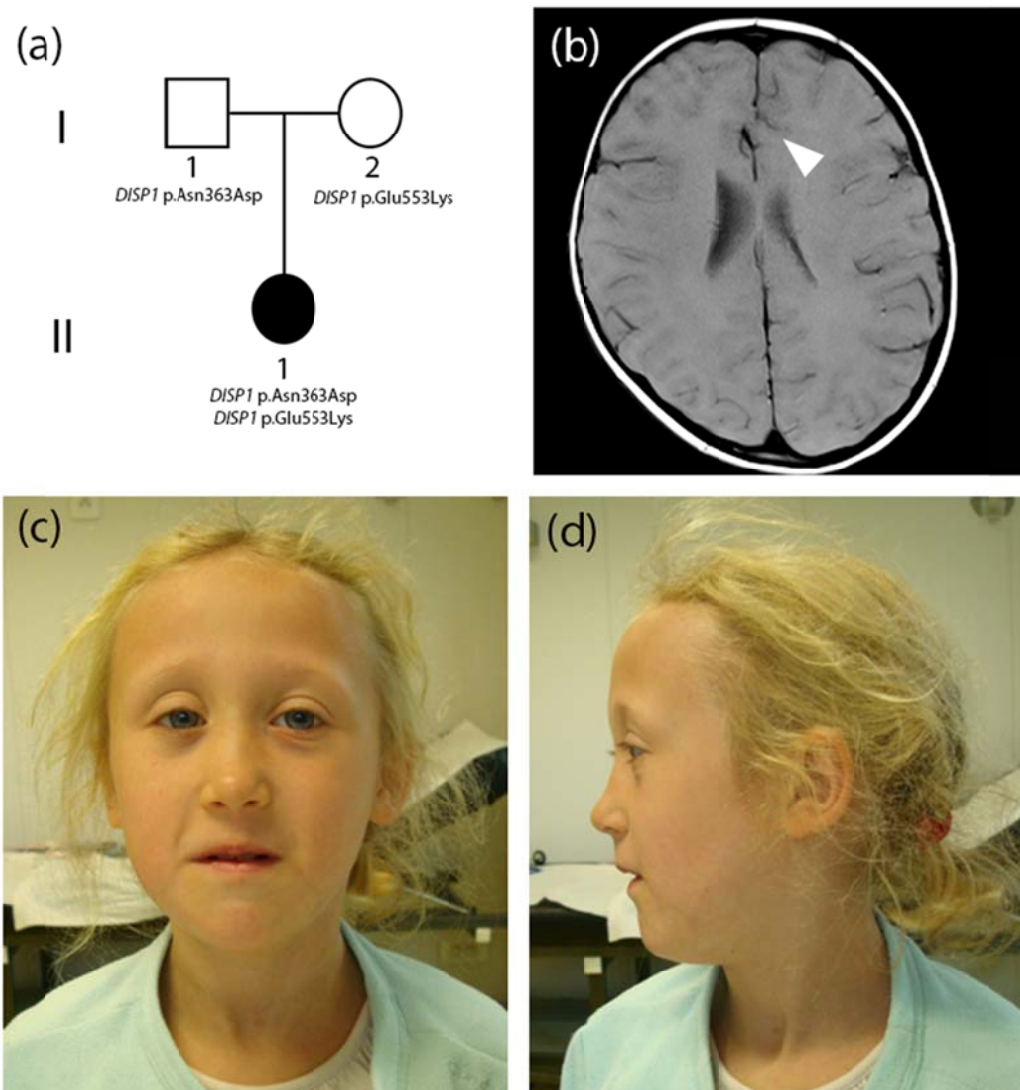


Figure 2. Pedigree of F2 family, and MRI of individual III1 of F2 family

(a) The F2 family consisted of 3 members. The daughter III1 has two *DISP1* compound heterozygous mutations, *DISP1* p.Asn363Asp, inherited from the father I1, and *DISP1* p.Glu553Lys, inherited from the mother I2. (b) Axial brain MRI of individual III1 of F2 family, harbouring a minor form of HPE, showing a very localized fusion of the hemispheres in the forebrain (white arrow). Facial (c) and lateral (d) photographs of the daughter III1 showing mild facial malformations.

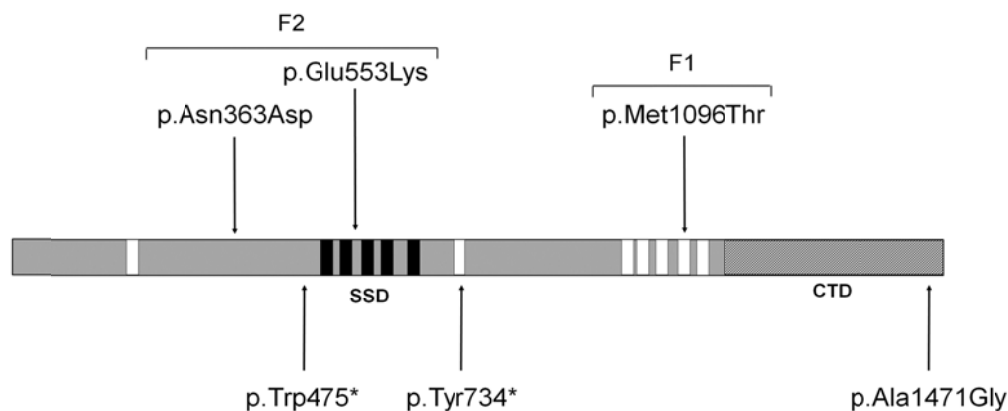


Figure 3. Distribution of all *DISP1* point mutations reported so far in HPE subjects

Mutations are shown on a schematic representation of *DISP1* protein. The white and black rectangles represent transmembrane helical domains, including the Sterol-Sensing Domain (SSD) from amino acid 486 to 658 (black). The hatched area is the C-terminal Domain (CTD, 360 last aminoacids of the protein). Mutations presented by families F1 and F2 are represented at the top, whereas mutations previously reported in the literature are represented at the bottom. The p.Trp475* and p.Tyr734* mutations were described by Roessler et al (38). The first mutation was present in a girl with seizures, developmental delay, midline cleft lip/palate and mild decortication, inherited from her mother. The second mutation was transmitted from a mother to her daughter who presents facial malformations: bilateral cleft lip/palate, hypotelorism, upslanting palpebral fissures and solitary maxillary central incisor. The p.Ala1471Gly mutation was reported by in a boy, born with heart abnormalities (ventricular septal defect and abnormal aorta), Bochdalek congenital diaphragmatic hernia and left-sided cleft lip with bilateral cleft palate (39).

Table 1. Characteristics of genes and mutations implicated in holoprosencephaly.

The mutation frequencies are given in qualitative terms: “High” is for genes mutated in more than 10% of HPE cases, “Medium” for genes mutated between 10% and 1%, and “Low” for genes mutated in less than 1% of HPE cases. Mutation frequencies were calculated based on our local HPE cohort (>1000 cases). Mainly inherited: inherited mutations from a parent are predominant among the reported cases; inherited: All reported mutations are inherited from a parent; NA: inheritance information was not available. CNV or large indels encompassing whole genes are not included in this table.

Table 2. Digenic inheritance in human HPE cases

Mutations are given in proteic nomenclature, except the del18p11 which carries the TGIF1 gene off.

Tables 3. Phenotypic description of families F1 and F2 members.

(a) Phenotypic description of family F1 members. The head circumferences of individuals harboring microcephaly are given in standard deviation (SD). Facial description of fetus III3 was not available (NA). The dash means that the phenotype is normal. (b) Phenotypic description of family F2 members. M=Male, and F=Female.

Table 4. Characteristics of *DISP1* and *SHH* mutations found in F1 and F2 families

Mutations reported in F1 family (*DISP1* p.Met1096Thr; *SHH* p.Pro347Gln) and in F2 family (*DISP1* p.Asn363Asp; *DISP1* p.Glu553Lys) were annotated using ANNOVAR. Minor alleles frequencies were extracted from dbSNP build 138, in the Exome Sequencing Project containing sequencing data from 6500 exomes (ESP6500), in the 1000 Genome Project release of 2014 (1000G), and in the Exome Annotation Consortium (ExAC) containing sequencing data from 60700 exomes. Bioinformatic predictions were given by 10 predictions tools (SIFT, PolyPhen-2 HDIV and HVAR, LRT, Mutation Taster, Mutation Assessor, FATHMM, Radial SVM, LR and CADD). The cumulated predictions were given here, D=Deleterious, P=Possibly Deleterious, T=Tolerated.

TABLES

Gene	Chromosomal Locus	Mutation frequency in nonsyndromic HPE	Percentage of Inherited mutations from a parent	Zygosity state	References
<i>SHH</i>	7q36	High (12%)	70%	Heterozygous	(5, 23, 45, 56-58)
<i>ZIC2</i>	13q32	Medium (9%)	30%	Heterozygous	(5, 45, 59-62)
<i>SIX3</i>	2p21	Medium (5%)	70%	Heterozygous	(5, 45, 63-67)
<i>TGIF1</i>	18p11.3	Medium (1,7%)	Mainly inherited	Heterozygous	(5, 68, 69)
<i>PTCH1</i>	9q22.3	Low	Mainly inherited	Heterozygous	(4, 70, 71)
<i>TDGF1</i>	3p23-p21	Low	NA	Heterozygous	(10)
<i>GLI2</i>	2q14	Low	Mainly inherited	Heterozygous	(70, 72, 73)
<i>DISP1</i>	1q42	Low	Mainly inherited	Heterozygous	(38, 39)
<i>FGF8</i>	10q24	Low	Mainly inherited	Heterozygous Homozygous	(11, 47)
<i>FOXH1</i>	8q24.3	Low	NA	Heterozygous	(74)
<i>NODAL</i>	10q22.1	Low	NA	Heterozygous	(75)
<i>GAS1</i>	9q21.33	Low	Mainly inherited	Heterozygous	(12)
<i>DLL1</i>	6q27	Low	Inherited	Heterozygous	(15)
<i>CDON</i>	11q24.2	Low	NA	Heterozygous	(13)
<i>STIL</i>	1p33	Low	Inherited	Heterozygous Homozygous	(8, 9, 76)

Table 1. Characteristics of genes and mutations implicated in holoprosencephaly.

Gene	Mutation	References
<i>SHH</i>	p.Gly290Asp	(23)
<i>ZIC2</i>	p.Ala461_Ala470dup	
<i>SHH</i>	p.Pro424Ala	(23)
<i>TGIF1</i>	del18p11	
<i>SHH</i>	p.del378_380	(23)
<i>TGIF1</i>	p.Thr151Ala	
<i>GLI2</i>	p.Arg151Gly	(70)
<i>PTCH1</i>	p.Thr328Ala	
<i>SIX3</i>	p.Ala93Asp	(4)
<i>PTCH1</i>	p.Ala393Thr	
<i>SIX3</i>	p.Ala284Pro	(77)
<i>ZIC2</i>	p.Trp304Arg	
<i>SHH</i>	p.Leu218Pro	(12)
<i>GAS1</i>	p.Asp270Tyr	
<i>SHH</i>	p.Cys363Tyr	(12)
<i>GAS1</i>	p.Asp288Gly	
<i>SHH</i>	p.Pro347Gln	In this report
<i>DISP1</i>	p.Met1096Thr	

Table 2. Digenic inheritance in human HPE cases

(a)

	Sex	Age	Brain MRI	Face
I1	M	81	Microcephaly (-5SD)	-
I2	F	79	-	-
II1	M	48	Microcephaly (-5SD)	-
II2	F	48	-	-
II3	M	46	Microcephaly (-4,5SD)	Hypotelorism
II5	M	42	-	-
II6	F	35	-	-
III1	M (fetus)	-	Semi-lobar HPE	Proboscis Macroglossy
III2	F (fetus)	-	Alobar HPE	Flat face hypotelorism Premaxillary agenesis Cleft lip/palate
III3	F (fetus)	-	Severe HPE	NA
III4	F	12	-	-
III5	F	11	-	-
III6	M	12	Microcephaly (-4SD)	Hypotelorism Cleft lip/palate
III7	M	11	Microcephaly (-3SD)	-
III8	F	9	-	-
III9	F	6	Microcephaly (-4SD)	-

(b)

	Sex	Age	Brain MRI	Face
I1	M	34	-	-
I2	F	33	-	-
II1	F	9	Lobar HPE Microcephaly (-2SD)	Flat face Short nose Hypotelorism Arched palate Cleft palate Microstomia Narrow palpebral fissures

Tables 3. Phenotypic description of families F1 and F2 members.

Gene	Nucleic acid change	Amino acid change	Minor Allele Frequencies				Bioinformatic predictions
			dbSNP	ESP6500	1000G	ExAC	
<i>DISP1</i>	c.T3287C	p.Met1096Thr	rs144673025	0,005	0,001	0,006	D:3 P:1 T:6
<i>SHH</i>	c.C1040A	p.Pro347Gln	-	0	0	0	D:9 P:1 T:0
<i>DISP1</i>	c.A1087G	p.Asn363Asp	-	0	0	0	D:7 P:2 T:1
<i>DISP1</i>	c.G1657A	p.Glu553Lys	-	0	0	0	D:5 P:1 T:4

Table 4. Characteristics of *DISP1* and *SHH* mutations found in F1 and F2 families